

The Occurrence and Enrichment of Scattered Indium: A Case Study of Dachang Ore Field in Guangxi, China

Pi Qiaohui^{1,2}, Lu Di², Yang Xiong², Yu Huidong²

¹Guangxi Key Laboratory of Hidden Metallic Ore Deposits Exploration, Guilin University of Technology, Guilin, China

²College of Earth Sciences, Guilin University of Technology, Guilin, China

Email address:

1481561260@qq.com (Pi Qiaohui)

To cite this article:

Pi Qiaohui, Lu Di, Yang Xiong, Yu Huidong. The Occurrence and Enrichment of Scattered Indium: A Case Study of Dachang Ore Field in Guangxi, China. *Earth Sciences*. Vol. 8, No. 6, 2019, pp. 303-316. doi: 10.11648/j.earth.20190806.11

Received: October 13, 2019; **Accepted:** November 8, 2019; **Published:** November 14, 2019

Abstract: The Dachang tin-polymetallic deposit, which is located in the northwestern part of the Guangxi Zhuang Autonomous Region, contains great amounts of indium. But the occurrence and enrichment of indium are rather complex and not yet well understood. In this paper, the Dachang West ore belt (Tongkeng, Gaofeng) sphalerite is taken as the research object. Based on detailed field investigation and indoor microscopic observation of mineral phase, the spatial distribution law, occurrence state and relationship with main metallogenic elements of scattered elements indium were studied by means of high-precision electron probe and plasma mass spectrometry, in order to reveal its enrichment in sphalerite. The study results show that the content of scattered elements indium in the sphalerite of the Tongkeng deposit decreases with the increase of depth, while the Gaofeng deposit remains stable. Indium occurs mainly in the form of isomorphism and enters sphalerite lattice in the form of double substitution of zinc with copper, but does not exclude the possibility of indium being deposited as a sub-microinclusions. On the basis of previous studies, it is inferred that the indium-rich and copper-rich fluids produced by magma crystallization are metasomatic and enriched with the early-formed sphalerite in the late evolution of Granite Magma. The results of this study point the way to mineral processing and the search for scattered elements indium.

Keywords: Dachang Tin-polymetallic Deposit, Indium, Isomorph, Occurrence and Enrichment of Indium

1. Introduction

Indium is a relatively rare metal with increasing economic importance in a variety of high-tech applications including photovoltaics, high-definition televisions, semiconductors, batteries, low-temperature solders, and liquid crystal displays [1-2]. However, the global annual production of indium is less than 570 tons [3-4]. Consequently, this upsurge of interest in indium has emphasized the need for improved understanding of the mineralogical distribution of indium and the factors controlling indium enrichment in ore.

In most cases, indium has a close relationship with tin, lead, zinc, and copper ore block [5-6], in which the tin-polymetallic ore block and massive sulfide ore block are two primary sources for indium [6-7]. In tin-polymetallic ore block, indium mainly occurs in the crystal lattice of marmatite form of sphalerite by isomorphism [8-9]. By contrast, in those ore block that with few sphalerite, indium is often hosted in tin sulfide mineral salts, for instance, the Portuguese Neves

Corvo tin-copper deposit contains stannite with indium levels of up to 0.7% [7]. However, independent minerals of indium have rarely been reported. Indium and copper can substitute for zinc [10-11], but only when the concentration of cadmium is within the “indium window” (0.2%–0.6%). Indium can metasomatize in a large number of marmatite lattices by isomorphism [12]. Spatially, indium has a close relationship with porphyritic dikes or rock beads formed during late-stage magma evolution [13-14], and indium is always enriched in metasomatic fluids and mixed indium-rich fluid and meteoric water [13-15].

The Dachang Sn-polymetallic ore deposit is one of the largest scale Sn ore block in the world, and is also an important source of indium and cadmium in China; the amount of indium is significant, up to 8795 tons [6]. Previous studies have mainly focused on Sn-polymetallic ore genesis [16-17], and the enrichment mechanisms of indium are poorly documented and understood [15-18].

This paper presents an integrated study of ore texture and

sphalerite geochemistry using typical samples from the Tongkeng and Gaofeng ore block in the Dachang tin-polymetallic sulfide ore block. The aim of this study was to assess the spatial distribution of indium in sphalerite, the occurrence state of indium, the relationship of indium with the main ore-forming elements, and to provide new insights as to how indium and related minor and trace elements can reach concentrations of several thousand ppm in some sphalerite-bearing ores.

2. Ore Deposit Geology and Ore Textures

2.1. Ore Deposit Geology

The Dachang Sn-polymetallic Ore-field is located in the Danchi Devonian rift basin that flanks the south-west border of the Jiangnan Massif, including the Lamo Cu-Zn skarns deposit, the Tongkeng Sn-Pb-Zn stratiform deposit and the GaoFeng massive sulfide ores deposit (Figure 1). Previous studies suggest that the west ore zone contain affluent rare earth element mineral resources [15]. The stratigraphical units

around the Dachang Ore-field consist of the Permian Qixia Group, the lower Carboniferous Shimen Group, the upper Carboniferous Huanglong Group, the Upper Devonian Tongcheijing Group, the Middle Devonian Liujiang Group, the Lower Devonian Cheihe Group. The Liujiang and Cheihe groups host most of the important mineralization.

The Main igneous rocks outcropped in the area are Longxianggai multiple-intruded pluton and granite porphyry or porphyritic diorite veins around the mine [19]. Longxianggai pluton, which is formed in three stages, can be divided into intrusive pluton of fine-grained porphyritic biotite granite (96.6 ± 2.5 Ma), the fine-grained biotite granite (94.3 ± 2.2 Ma) and porphyritic biotite granite (93.8 ± 0.84 Ma), in which fine-grained biotite granite and tin polymetallic ore are most closely related [20]. Near and within the Changpo mine area both granitic and quartz-plagioclase porphyritic-diorite dikes (91.3 ± 1.2 Ma) occur, shows close relationship between them and the mineralization. The dikes generally exhibit mild sericitic quartz hydrothermal alteration and are relatively low in Sn.

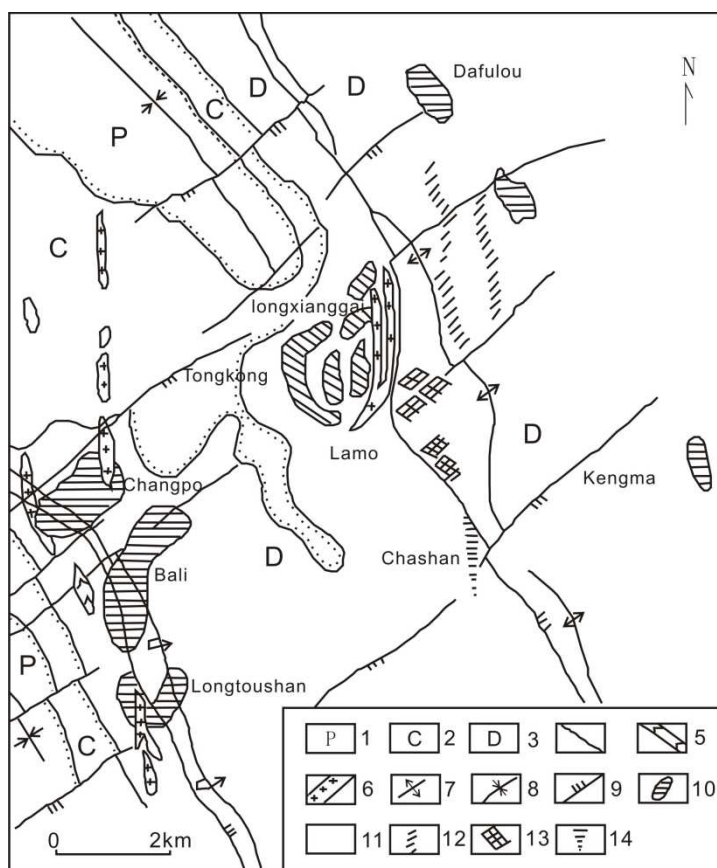


Figure 1. Mineralization zone of Dachang ore field (compiled from China Nonferrous Metals Industry Corporation, 1987): 1-Permian limestone and siliceous; 2-Carboniferous limestone; 3-Devonian limestone, shale and siliceous; 4-Parallel unconformity stratigraphic contact; 5-Diorite porphyrite; 6-Granite and granite porphyry; 7-Anticline axis; 8-Syncline axis; 9-Faults; 10-Tin orebody; 11-Zn-Cu orebody; 12-Scheelite veins; 13-Wolframite veins; 14-Antimony veins.

The NW-trending Longxianggai anticline and Longxianggai fault and the Dachang anticline and Dachang fault paralleled each other are main structural systems in the area. The anticlines are asymmetrical with a steeply dipping to SW limb and a gentle dipping to NE limb and overturned

locally.

TongKeng deposit, the major mine in the Dachang deposit, contains three types of ore bodies hosted within Upper Devonian siliceous rocks and limestones (D^3). Vein and stockwork-type ore bodies, comprise the large No. 2, occur in

the upper part of the deposit, Stratiform and bedded ore bodies occur in the lower part of the deposit and comprise the large No. 92. A skarn-type Cu–Zn orebody, beneath the Changpo orebody, occurs adjacent to the Longxianggai granite and comprise the large No. 95 or 96, The Longtaoshan No. 105

stratiform cassiterite-sulfide orebody of GaoFeng deposit is hosted by Middle Devonian reef limestones and contains massive sulfides that constitute the highest grade ores in the DaChang deposit.

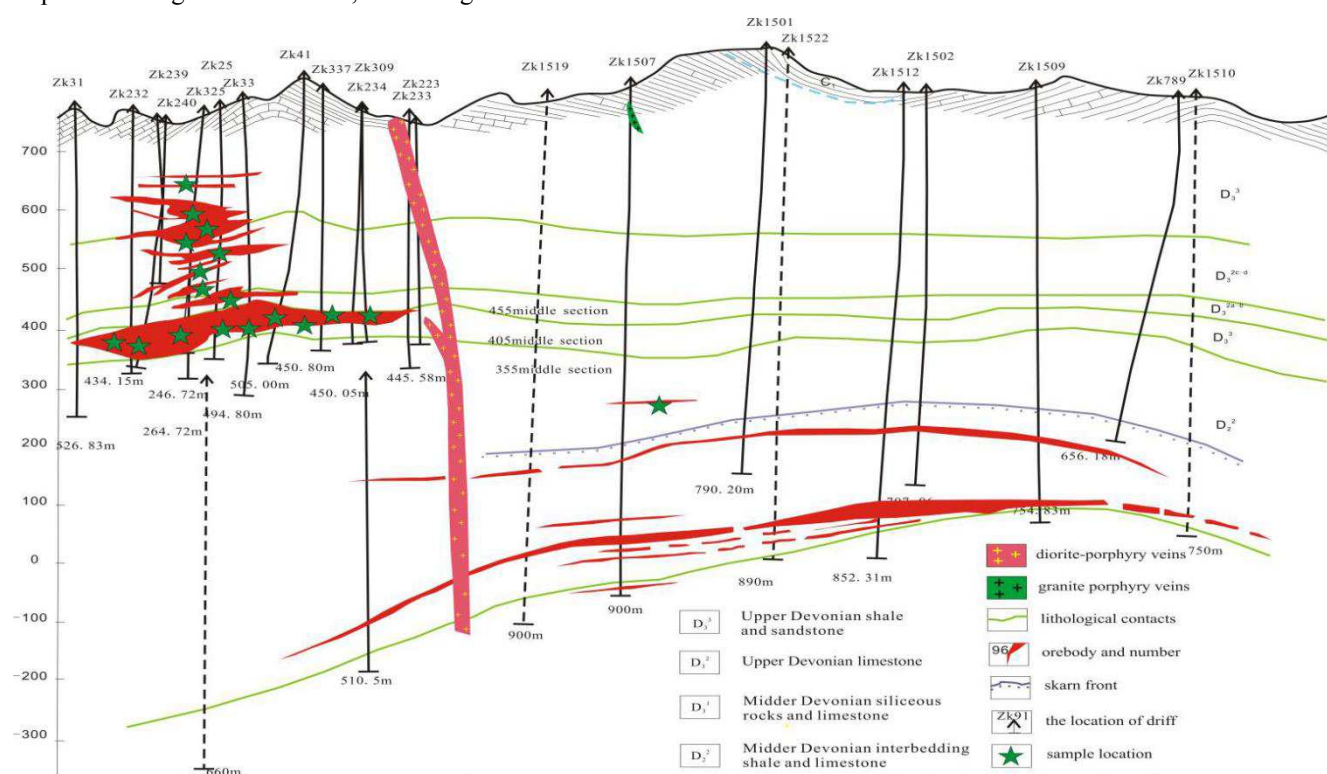


Figure 2. The location of samples in Tong-Keng deposit of DaChang (modified from No. 215 Geological Team of Guangxi HuaXi Group).

2.2. Ore Textures

2.2.1. GaoFeng Deposit

Orebody No. 105 of the Gaofeng deposit has average concentrations of 2.5% Sn, 9.7% Zn, 4.8% Pb, 4.2% Sb, and 225 g/t Ag. The deposit is aligned north–south along strike, and has an overall dumbbell-like shape, large at both ends and small in the middle. The central orebody is crosscut by granite porphyry. Field observations and thin-section observations show consistent vertical and laterally variable ore mineral assemblages in orebody No. 105. The mineral assemblages in the northern part mainly include cassiterite, arsenopyrite, marmatite, and pyrrhotite. The arsenopyrite is euhedral and has cracks filled by cassiterite, pyrrhotite, and more arsenopyrite, indicating that the euhedral arsenopyrite formed earlier (Figure 3A).

The mineral assemblages around the central granite porphyry contain marmatite, pyrrhotite, and chalcopyrite, mainly as infillings resulting from metasomatism. The marmatite crystals are euhedral, and are isolated residues replaced by pyrrhotite. Chalcopyrite is xenomorphic in pyrrhotite, and some chalcopyrite is found infilling fractures in sphalerite (Figure 3B–C). The mineral assemblages in the southern orebody contain jamesonite, marmatite, pyrrhotite, and calcite, mainly from infilling and metasomatism. Pyrrhotite and calcite are replaced by each other, and

replacement of pyrrhotite by jamesonite is present, indicating that jamesonite was the final stage (Figure 3D).

The main periods of mineralization in the ore block. The earlier was the main mineralization, there are chalcopyrite rich in the late metallogenic period, pyrite assemblage in the form of metasomatism and vein intercalation in the early sphalerite minerals. At the same time, chalcopyrite is produced from sphalerite in droplet form.

2.2.2. TongKeng Depoite

The mineral assemblage in the middle level 255 of orebody No. 95 contains chalcopyrite, marmatite, pyrrhotite, and calcite, all having a paragenetic relationship and indicating that they were simultaneously formed (Figure 3E). The middle level 405 of orebody No. 92 includes stockwork tin-lead-zinc orebodies, chalcopyrite distributed as irregular shapes in sphalerite, and pyrite veinlets that infilling sphalerite cleavage (Figure 3F). The middle level 455 of No. 92 orebody contains tin-lead-zinc orebodies, euhedral pyrite replaced by sphalerite, and late chalcopyrite infilling fissures in sphalerite (Figure 3G). The middle level 505 of No. 92 orebody contains tin-lead-zinc orebodies. Late chalcopyrite infills fractures and joints in sphalerite, sphalerite is interspersed with xenomorphic pyrite veinlets, vein chalcopyrite is interspersed in sphalerite, and crossed veinlets are visible in coarse veins of the same stage, indicating that vein chalcopyrite formed after

the sphalerite stage, and pyrite and chalcopyrite formed during the same stage (Figure 3H). The middle level 584 of No. 2 orebody contains tin-lead-zinc orebodies, xenomorphic cracked pyrite replaced by pyrrhotite, jamesonite infilling pyrrhotite, and pyrite with a smooth interface and no obvious metasomatism, (indicating that the jamesonite formed significantly later than pyrrhotite and pyrite), and chalcopyrite infilling gaps in pyrite and pyrrhotite (Figure 3I).

The formation of the Tongkeng deposit included a skarn stage, a cassiterite sulfide stage, and a copper-rich sulfide stage. The skarn stage, which contains mainly chalcopyrite and sphalerite, occurs in the No. 95 zinc-copper orebody. The

cassiterite sulfide stage, which mainly includes cassiterite, pyrite, pyrrhotite, and marmatite, is found in orebodies No. 91 and No. 92. The copper-rich sulfide stage, which contains chalcopyrite, pyrite, jamesonite, and calcite, is found in deep orebody No. 92 as infilling and metasomatism. Therefore, at least two stages of chalcopyrite and pyrite are present. Early lumpy chalcopyrite is associated with sphalerite, and late star-shaped and vein chalcopyrite infills early sphalerite. The situation is similar for pyrite. The Gaofeng and Tongkeng ore block have similar textural and structural characteristics, and in both ore block late-stage copper-rich fluid infilled and replaced main-stage sphalerite.

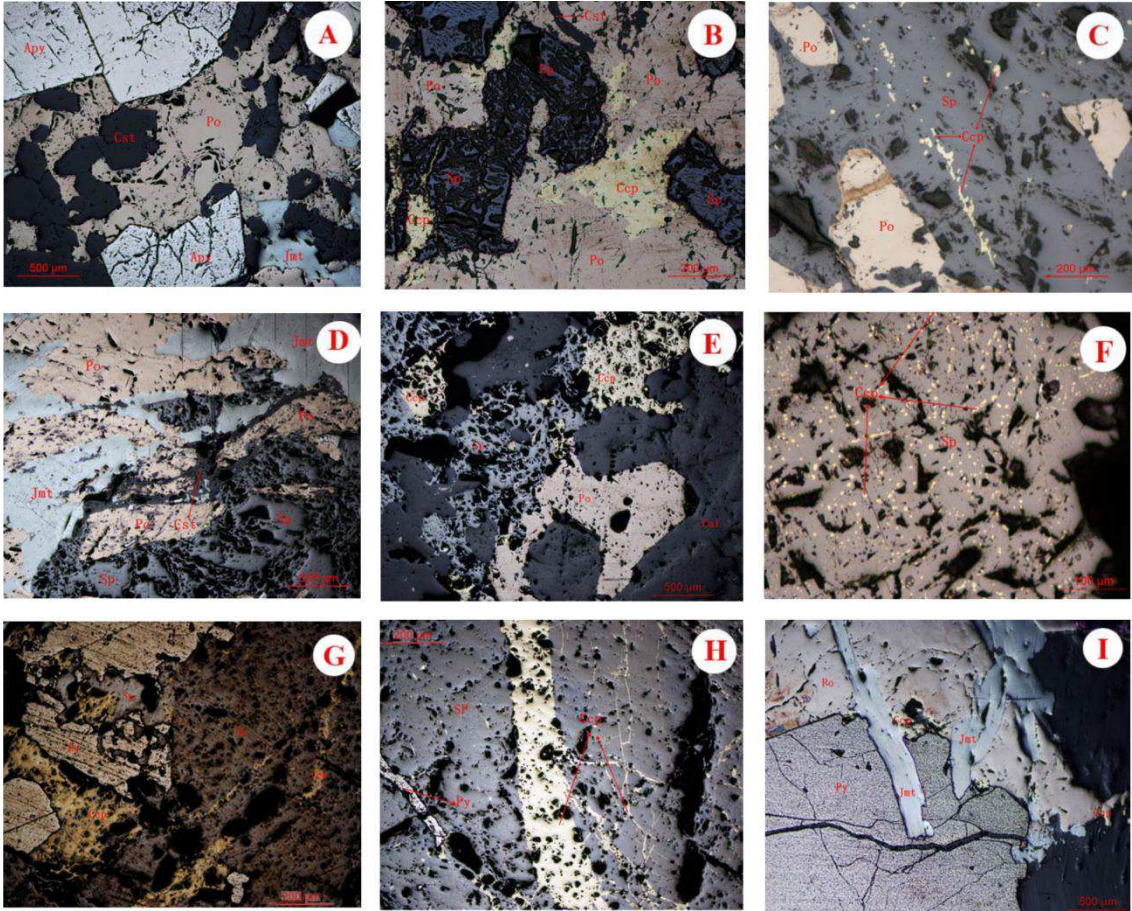


Figure 3. Photomicrographs in reflected light illustrating textures and structures in the tin-polymetallic ore of GaoFeng and Tong-Keng deposit. A: mineral assemblages and textures of in the Northern of the tin-polymetallic ore of No. 105. B-C: mineral assemblages and textures of beside granite porphyry in the tin-polymetallic ore of No. 105. D: mineral assemblages and textures of in Southern of the tin-polymetallic ore of No. 105. E: mineral assemblages and textures of on the level 255 m the zinc-copper of No. 95. F: mineral assemblages and textures of on the level 405 m the tin-polymetallic ore of No. 92. G: mineral assemblages and textures of on the level 455 m the tin-polymetallic ore of No. 92. H: mineral assemblages and textures of on the level 505 m the tin-polymetallic ore of No. 92. I: mineral assemblages and textures of on the level 584 m the tin-polymetallic ore of No. 2.

Table 1. Overview of samples investigated, mineral assemblages and key ore textures.

Desposite, Sample No	Orebaby, Location,	Ore assemblage	Ore textures
Tong-Keng deposit			
TK95-1	skarn-type Cu–Zn orebody of No. 95, level 255 m	Py, Sp, Ccp, Po	Exsolution of Cp in Sp; Fine-grained; late replacement of Sp by Py
TK92-7	Layer of massive Sn–Pb–Zn ore of No. 92, level 381 m	Py, Sp, Po, Q	euhedral pyrite are replaced by sphalerite
TK92-4	Layer of massive Sn–Pb–Zn ore of No. 92, level 381 m	Py, Sp, Po	infillment and replacement of apy by Sp and Po
TK92-1	Layer of massive Sn–Pb–Zn ore of No. 92, level 405 m	Py, Sp, Q, Cst	infillment and replacement of py by Sp and Q;
TK92-6	Layer of massive Sn–Pb–Zn ore of No. 92, level 455 m	Py, Sp, Po, Q, Cst	infillment and replacement of apy by Sp and Po
TK92-18	Layer of massive Sn–Pb–Zn ore of No. 92, level 455 m	Py, Sp, Po, Apy	infillment and replacement of apy by Sp and Q;

Desposite, Sample No	Orebody, Location,	Ore assemblage	Ore textures
TK190-1	Layer of massive Sn-Pb-Zn ore of No. 190, level 505 m	Py, Sp, Jmt	infillment and replacement of apy by Jmt; Ccp as inclusions in Sp
TK2-7	Vein of Sn-Pb-Zn ore of No. 2, level 585 m	Py, Sp, Jmt, Apy	Marginal corrosion of Py, Apy with Replacement of Sp, Jmt; Ccp as infillment among Sp, Py, Apy
GaoFeng depoite	Layer of massive Sn-Pb-Zn ore of No. 105		
GF105-1	Southern of ore in the level -200 m	Sp, Po, Jmt	exsolutions of Ccp in Sp; Ccp replacement along cleavages in Sp
GF105-4	Middle of ore in the level -151 m, beside of granite porphyry	Sp, Po, Cst	exsolutions of Ccp in Sp; Ccp replacement along cleavages in Sp
GF105-7	Middle of ore in the level -200 m	Sp, Po, Cst	Marginal corrosion of Po with Replacement of Sp
GF105-11	Northern of ore in the level -200 m	Sp, Po, Cst	Marginal corrosion of Po with Replacement of Sp
GF105-17	Middle of ore in the level -151 m, Northern of oil tank	Sp, Po, Py	exsolutions of Ccp in Sp; Ccp replacement along cleavages in Sp
GF105-19	Northern of ore in the level -151 m	Sp, Po, Py	exsolutions of Ccp in Sp; Ccp replacement along cleavages in Sp
GF105-22	Middle of ore in the level -103m; Northern of granite porphyry	Sp, Po, Py	infillment and replacement of apy and Cst by Sp
GF105-23	Middle of ore in the level -103 m	Sp, Po, Py, Jmt	infillment and replacement of apy and Cst by Sp
GF105-30	Southern of ore in the level -103 m	Sp, Po, Py, Jmt	Marginal corrosion of Apy with Replacement of Sp and Jmt

3. Sample and Analytical Methods

To study the Dachang western belt (Gaofeng, Tongkeng) spatial variation of indium Concentrations, we get the samples in different levels of two deposits. For instance, 255, 381, 405, 455, 505, 584 level in Tongkeng deposit, sampling locations are shown in Figure 3, -103, -151, -200 leves in 105# orebody of Gaofeng deposit, due to 105# orebody complex morphology, it's difficult to be shown in figure. Sample description and sampling locations are shown in Table 1. Tongkeng deposit samples in 92[#], 95[#], 190[#], 2[#] orebody. 95[#] orebody is stratiform skarn orebody, 190[#] orebody is hosted in Dachang fault, 92[#] orebody is the biggest stratiform sulfide orebody in Tongkeng deposit, 2[#] orebody is thin vein cassiterite-sulphide deposit. 105[#] orebody in Gaofeng deposit is similar to 100[#] orebody, are late filling organic reef limestone massive sulfide orebodies.

Sphalerite is the main component in all the studied ore block. The suite of samples is representative of the different deposit types. Sample descriptions are given in Table 2, and sampling locations are marked on Figure 2.

After identified ore specimens, the polishing thin section were observed in microscope, accompanied in State Key Laboratory of Ore Deposit Geochemistry. Electron microprobe analyses were carried out using (JEOL) JXA-8230 electron microprobe at the Guangxi Key Laboratory of Hidden Metallic Ore Deposits Exploration. Trace element analysis of sphalerite was performed the Geophysical and Geochemistry Exploration Institute of the Chinese Academy of Geological Sciences laboratory, the analytical methods was similar to Ye et al. [10].

4. Results

4.1. Minor and Trace Element Concentrations

The results of trace element analysis of sphalerite are summarized in Table 2 and Figure 4. As skarn orebody No. 95 lacks sphalerite, we used the Lamo deposit as a

comparison. The concentrations of Fe, Mn, and Cd are constant, while the concentrations of In, Cu, Pb, Sn, Bi, and Sb significantly vary.

4.1.1. Indium, Cadmium, and Gallium

A remarkable feature of the data for Fe and Mn is that the concentrations of these elements are relatively constant in each sample. The concentration of Fe ranges from 11.98% to 16.25%, with a mean value of 13.45%, indicating it belong to the in marmatite [10]. The In concentration ranges from 774×10^{-6} to 1265×10^{-6} , with a mean value of 998×10^{-6} . The In concentrations in the Tongkeng deposit are the highest and relatively stable. In Gaofeng orebody No. 105, the Cd concentration is relatively constant, ranging from 3484×10^{-6} to 4475×10^{-6} , with a mean value of 4215×10^{-6} , while the concentration of gallium is low, ranging from 7.4×10^{-6} to 26.6×10^{-6} , with a mean value of 9.8×10^{-6} .

4.1.2. Tin, Lead, Copper, and Antimony

The concentrations of Sn, Pb, Cu, and Sb vary over several orders of magnitude. The Sn concentration ranges from 8.8×10^{-6} to 2465×10^{-6} , with a mean value of 1265×10^{-6} . The Sn levels are very high in the Gaofeng deposit, indicating that the deposit may contain tin inclusions. The Sn concentrations in the Lamo deposit are under the limit of detection. The Pb levels range from 39.4×10^{-6} to 12351×10^{-6} , with a mean value of 2134×10^{-6} , indicating lead-rich inclusions or an independent mineral in sphalerite. The concentration of copper ranges from 502×10^{-6} to 2728×10^{-6} , with a mean value of 1365×10^{-6} , indicating that sphalerite may contain chalcopyrite as tiny inclusions or an independent mineral. The Cu concentration is highest in the Lamo deposit, with a mean value of 7920×10^{-6} . The Cu concentrations in the Gaofeng deposit and the Tongkeng deposit are similar. The levels of Sb vary from 38.0×10^{-6} to 12100×10^{-6} , are lower in the Tongkeng deposit and Lamo deposit, and the highest value in the Gaofeng deposit is 12100×10^{-6} , indicating that this sample might contain stibnite.

4.1.3. Bismuth, Titanium, and Nickel

The concentrations of Bi, Ti, and Ni are lower and significantly vary. The Bi concentrations range from 0.09×10^{-6} to 63.5×10^{-6} , with the highest values observed in the Tongkeng deposit and the lowest in the Gaofeng deposit, indicating that the sphalerite in the Tongkeng deposit may contain bismuth copper ore and tiny inclusions of bismuthinite. The concentrations of Ti and Ni are lower and vary significantly, from 3.28×10^{-6} to 55.8×10^{-6} and 1.35×10^{-6} to 7.88×10^{-6} , respectively, and may isomorphically occur.

4.1.4. Cobalt, Chromium, Thallium and Arsenic

The concentrations of Co and Cr are low, ranging from 0.38

$\times 10^{-6}$ to 172×10^{-6} and 8.04×10^{-6} to 19.2×10^{-6} , respectively, and isomorphically occur. The Co levels in sphalerite in the Lamo deposit are up to 172×10^{-6} , indicating the presence of cobaltite enclaves. The As concentration significantly varies, from 27.9×10^{-6} to 9016×10^{-6} , with the highest levels in the Tongkeng deposit and the Gaofeng deposit, indicating replacement of S by As in sphalerite. The Tl levels are lower, less than 1×10^{-6} .

The concentrations of trace elements in sphalerite are high, particularly Fe, Mn, Cd, In, Sn, Pb, Cu, and Sb. The concentrations of Fe, Mn, and Cd are relatively stable and those of In, Sn, Pb, Cu, and Sb significantly vary.

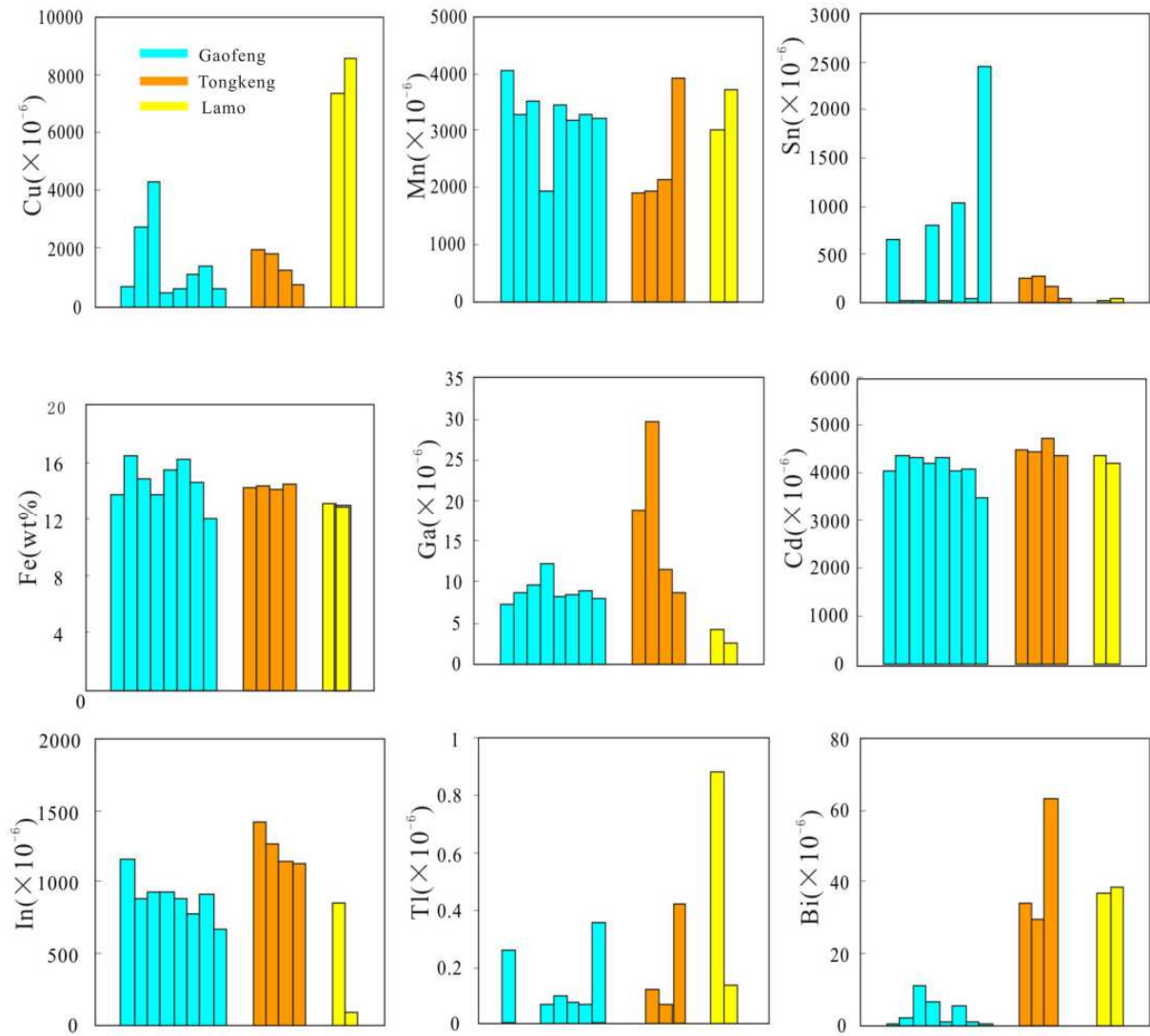


Figure 4. Histograms showing the Variation of trace elements Concentrations for sphalerite.

Table 2. Analytical result of trace elements for sphalerite of the DaChang Mine ($\times 10^{-6}$).

	Li	Cr	Mn	Co	Ni	Cu	Zn	Ga	Rb	Sr	Mo	Cd	In	Cs	Ba	Tl
GaoFeng deposit																
GF105-1	29.3	8.04	4059	1.43	1.94	662	525350	7.40	23.0	1.14	0.60	4045	1153	8.56	21.8	0.26
GF105-7	3.24	12.7	3282	0.66	2.63	2718	508151	8.70	0.88	-	4.81	4389	884	0.43	4.37	-
GF105-9	3.43	10.8	3514	0.48	2.24	4320	536816	9.72	0.77	7.54	0.41	4336	934	0.32	3.86	-
GF105-17	5.44	17.9	3834	0.43	4.14	502	536522	12.3	0.57	0.40	0.71	4125	504	0.19	8.73	0.07
GF105-19	10.3	15.8	3453	0.43	3.46	610	524566	8.14	6.54	-	0.34	4334	881	1.94	8.52	0.10

	Li	Cr	Mn	Co	Ni	Cu	Zn	Ga	Rb	Sr	Mo	Cd	In	Cs	Ba	Tl
GF105-22	10.9	11.8	3176	0.38	2.65	1092	483798	8.55	6.93	-	0.47	4058	774	2.30	11.8	0.08
GF105-23	12.2	12.7	3284	0.39	2.48	1420	518294	9.01	7.59	0.07	0.41	4090	912	2.34	17.3	0.07
GF105-30	56.6	12.2	3227	0.90	2.82	597	440482	8.00	31.4	0.22	4.86	3484	671	11.0	31.1	0.35
TongKeng deposit																
TK92-4	2.13	13.0	1905	4.04	2.36	1938	551418	18.9	0.58	0.16	0.51	4475	1421	0.20	10.8	-
TK92-6	2.36	16.6	1946	5.52	7.88	1787	542402	29.6	0.86	0.74	2.63	4449	1265	0.52	7.83	0.12
TK92-7	1.62	9.63	2149	0.44	1.35	1220	542010	11.6	0.32	0.13	0.09	4718	1148	0.09	17.0	0.07
TK92-18	41.5	19.2	3912	1.42	3.26	781	528682	8.75	26.4	4.11	0.39	4388	1135	10.7	25.5	0.42
LaMo deposit																
LM-3	7.70	16.2	3008	172	5.11	7316	521332	4.11	125	0.59	2.63	4350	868	156	4.27	0.88
LM-6	4.47	11.8	3701	20.8	3.92	8525	519608	2.51	5.50	1.48	0.71	4222	92.9	0.83	5.57	0.14

	Pb	Bi	Th	U	Nb	Ta	Zr	Hf	Sn	Sb	Ti	W	As	V	Sc	Y
GaoFeng deposit																
GF105-1	39.4	0.09	0.28	1.02	0.09	0.28	1.14	-	650	38.0	17.2	0.89	916	15.0	1.11	0.40
GF105-7	212	2.03	0.13	1.66	0.09	0.10	1.45	-	8.88	238	3.28	0.13	9011	11.0	1.10	0.20
GF105-9	838	10.7	0.16	1.98	0.06	0.06	0.85	-	13.2	709	4.67	0.40	416	9.84	1.18	0.32
GF105-17	12351	6.26	<0.05	0.10	0.13	0.31	0.20	-	806	12100	1.61	0.79	27.9	5.76	3.19	0.12
GF105-19	64.4	0.62	0.09	2.15	0.06	0.10	0.43	-	15.0	44.7	7.13	0.42	97.5	11.9	0.84	5.51
GF105-22	289	5.19	<0.05	0.85	0.09	0.07	0.19	-	1035	262	3.60	1.00	281	11.4	1.61	0.88
GF105-23	2926	0.88	0.13	1.05	0.13	0.19	0.79	-	31.5	2423	27.4	0.94	176	11.6	0.76	1.24
GF105-30	426	0.15	0.07	0.89	0.10	0.06	0.30	-	2451	450	11.8	4.22	3076	14.0	1.36	0.45
TongKeng deposit																
TK92-4	162	33.9	<0.05	-	0.08	0.09	0.73	-	251	106	6.25	0.99	310	9.94	1.02	0.07
TK92-6	79.8	29.7	<0.05	-	0.13	0.09	0.61	-	259	58.7	14.2	0.53	4156	11.8	1.49	0.30
TK92-7	109	63.5	<0.05	-	0.08	0.08	0.15	-	159	48.4	4.62	0.83	179	10.2	0.75	0.05
TK92-18	52.4	0.15	0.09	0.65	0.13	0.08	1.48	0.05	32.2	45.6	38.2	0.40	1372	22.6	1.58	0.31
LaMo deposit																
LM-3	59.6	37.1	0.34	0.06	0.36	0.18	2.87	0.07	16.2	53.4	55.8	3.18	140	12.5	2.26	1.52
LM-6	716	38.6	0.30	0.39	0.33	0.18	12.6	0.32	27.8	89.4	38.5	10.5	311	6.97	1.06	0.95

4.2. Spatial Variation in Indium Concentration

Using electron microprobe data from middle levels 584, 505, 405, 381, and 255 of the Tongkeng deposit and middle levels -200, -151, and -103 of the Gaofeng deposit, a histogram was constructed showing the analytical results plotted against depth (Figure 5). The spatial distribution of sphalerite in the Tongkeng and Gaofeng ore block is as follows:

4.2.1. Tongkeng Deposit

The concentration of In in sphalerite in different orebodies varies markedly. The level in skarn zinc-copper orebody No. 95 is the lowest, ranging from 0.00% to 0.068%, with a mean value of 0.022%. The concentration of In ranges from 0.034%–0.098% in 381 middle stratiform tin polymetallic orebody No. 92, with a mean value of 0.070%; the concentration in middle level 455 of stratiform tin polymetallic orebody No. 92 is the highest, ranging from 0.036%–0.170% with a mean value of 0.109%; the In concentration in sphalerite from vein tin polymetallic metal orebody No. 2 ranges from 0.089%–0.113%, with a mean value of 0.098%; and that of sphalerite in the country rock ranges from 0.003%–0.010%, with a mean value of 0.007%.

The concentration of Cu in sphalerite is similar to In. In middle level 455 of stratiform tin polymetallic orebody sphalerite No. 92 the concentration is up to 2.893%, with a mean value of 0.253%. Skarn zinc-copper orebody No. 95 has a minimum of 0.034% and an average of 0.145%. The concentration of tin in sphalerite is low, under the limit of

detection. Differently from Cu, the In, Cd, and Fe concentrations in sphalerite show some variation. In the Tongkeng deposit, sphalerite Cd concentrations are around 0.4%–0.5%, and Fe concentrations are around 10%–11%.

4.2.2. Gaofeng Deposit

The In concentrations of sphalerite in No. 105 orebody are uniform, mostly 0.08%–0.11%, with the highest value being 0.133% and the lowest 0.047%. The values in sphalerite near the granite porphyry are slightly higher. Cd levels range from 0.420%–0.630%, with a mean value of 0.509%. Fe concentrations range from 9.755%–12.904%, with a mean value of 11.13%. The Cu concentrations range from 0.035%–0.447%, with a mean value of 0.097%. The In and Cd concentrations of sphalerite are similar in orebody No. 105 of the Gaofeng deposit and orebody No. 92 of the Tongkeng deposit.

4.2.3. Spatial Distribution

The In levels in sphalerite in the Tongkeng deposit decrease with increasing depth, and show a close relationship with the lithophile elements Cu and Sn. Cd and Fe concentrations are stable and independent of depth and location. The In and Cd levels in sphalerite in the Gaofeng deposit No. 105 orebody remain constant.

4.3. Concentration Maps of Indium and Relate Elements in Sphalerite

Based on electron microprobe analysis, we used locations with high In concentrations to study the distributions of In, Cd, and associated main ore-forming elements. We selected three

different regions to analyze the surface distribution of In and related elements in sphalerite (Figure 6).

As shown in Figure 6, In, Cd, Cu, and Sn have different distributions in sphalerite. A large amount of In occurs isomorphically in sphalerite at levels lower than those of Cd, Cu, and Sn, such as samples GF105-24 and TK92-1. However, very few samples have significantly high In concentrations and the distribution is very uneven, associated with the emergence of points with high In concentrations (arrows in Figure 6), such as sample TK190-1. Determining whether these points with high In concentrations represent In-rich

nanometer-scale inclusions will require further research.

There are two types of distribution of copper in sphalerite: isomorphic (which is evenly distributed) and as fine inclusions such as sample TK92-1. The fine inclusions have grain diameters of around 1 μm , and the copper distribution in the sphalerite of sample TK190-1 is similar to that of indium and tin. Tin distribution in sphalerite is of three types: isomorphic (which is evenly distributed), such as sample GF105-24; fine inclusions, such as sample TK92-1, in which the inclusions have grain diameters of around 1 μm ; and in bands, such as sample TK190-1. Cadmium in sphalerite occurs mainly isomorphically.

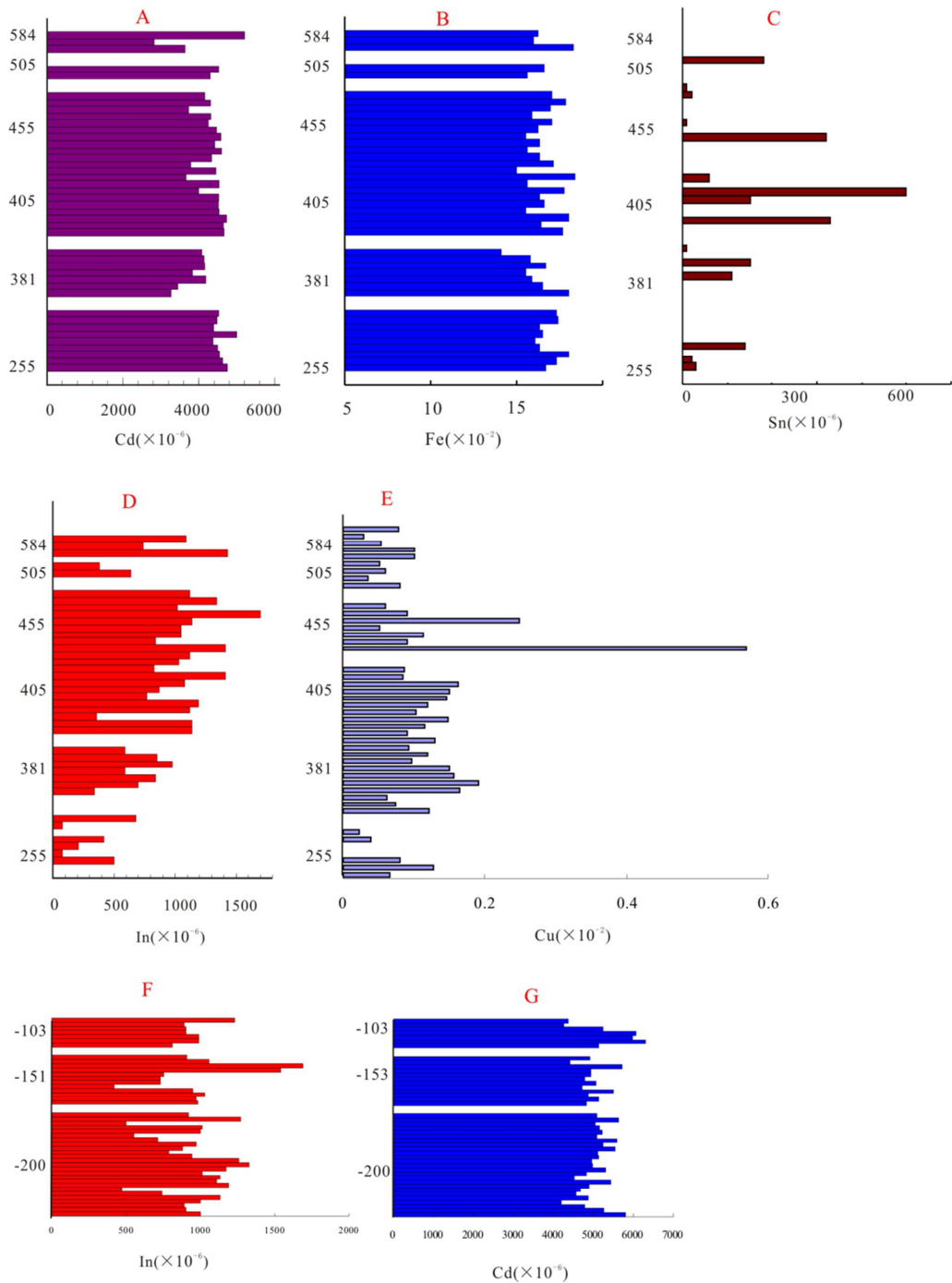


Figure 5. Histograms showing the Variation of In, Cd, Cu, Fe, Sn Concentrations for sphalerite of TongKeng and GaoFeng deposit in different levels.

Table 3. Summary of EMPA data for sphalerite by deposit and sample (%).

	As	Cu	Sn	In	Cr	S	Zn	Ni	Cd	Fe
TongKeng deposit										
The Sample from skarn-type Cu–Zn orebody of No 95, level 255 m										
MEAN (9)	0.006	0.145	0.002	0.022	0.010	33.360	52.640	0.008	0.475	11.443
S.D.	0.010	0.101	0.005	0.025	0.009	0.718	0.591	0.005	0.026	0.485
MIN	0.000	0.034	0.000	0.000	0.000	32.302	51.381	0.000	0.443	10.943
MAX	0.028	0.354	0.014	0.068	0.024	34.018	53.220	0.014	0.520	12.491
The Sample from Layer of massive Sn-Pb-Zn ore of No 92, level 381 m										
MEAN (7)	0.006	0.217	0.004	0.070	0.003	33.114	54.254	0.013	0.444	9.687
S.D.	0.011	0.295	0.006	0.021	0.005	0.428	0.522	0.006	0.049	0.929
MIN	0.000	0.052	0.000	0.034	0.000	32.516	53.509	0.010	0.365	8.185
MAX	0.030	0.869	0.015	0.098	0.010	33.807	55.120	0.022	0.523	10.456
The Sample from Layer of massive Sn-Pb-Zn ore of No 92, level 405 m										
MEAN (11)	0.011	0.253	0.007	0.108	0.005	33.509	53.190	0.006	0.466	10.863
S.D.	0.016	0.606	0.014	0.027	0.007	0.642	1.089	0.008	0.037	0.782
MIN	0.000	0.061	0.000	0.036	0.000	32.508	50.930	0.000	0.401	9.170
MAX	0.040	2.893	0.050	0.150	0.021	34.980	55.443	0.024	0.537	11.841
The Sample from Layer of massive Sn-Pb-Zn ore of No 92, level 455 m										
MEAN (10)	0.010	0.243	0.007	0.112	0.005	33.609	53.090	0.006	0.446	10.863
S.D.	0.006	0.506	0.014	0.023	0.007	0.742	1.079	0.008	0.047	0.742
MIN	0.000	0.061	0.000	0.076	0.000	32.408	50.960	0.000	0.301	9.270
MAX	0.030	2.693	0.050	0.170	0.021	34.880	55.433	0.024	0.537	11.641
The Sample from Layer of massive Sn-Pb-Zn ore of No 190, level 505 m										
MEAN (3)	0.005	0.091	0.000	0.109	0.010	32.649	55.084	0.000	0.474	9.726
S.D.	0.008	0.033	0.000	0.035	0.008	0.312	2.866	0.000	0.050	3.030
MIN	0.000	0.065	0.000	0.074	0.002	32.425	51.949	0.000	0.441	7.062
MAX	0.014	0.128	0.000	0.143	0.018	33.006	57.569	0.000	0.532	13.022
The Sample from Layer of massive Sn-Pb-Zn ore of No 2, level 585 m										
MEAN (4)	0.005	0.075	0.005	0.098	0.005	33.144	52.964	0.009	0.478	10.989
S.D.	0.0070	0.0229	0.0091	0.0097	0.0081	0.4083	0.7944	0.0071	0.0382	0.8403
MIN	0.000	0.057	0.000	0.089	0.000	32.565	51.798	0.001	0.42	9.877
MAX	0.017	0.114	0.021	0.113	0.019	33.709	53.896	0.019	0.527	12.148
GaoFeng deposit										
The Sample from Layer of massive Sn-Pb-Zn ore of No 105, level -200 m, beside										
MEAN (20)	0.013	0.102	0.003	0.095	0.007	32.965	53.358	0.009	0.510	11.039
S.D.	0.023	0.085	0.006	0.025	0.014	0.703	1.447	0.008	0.031	1.124
MIN	0.000	0.035	0.000	0.047	0.000	32.139	51.036	0.000	0.452	9.018
MAX	0.08	0.447	0.026	0.133	0.062	34.826	55.678	0.024	0.564	12.752
The Sample from Layer of massive Sn-Pb-Zn ore of No 105, level -200 m										
MEAN (6)	0.001	0.069	0.006	0.077	0.003	33.534	52.141	0.006	0.498	11.718
S.D.	0.001	0.019	0.009	0.019	0.004	0.426	0.462	0.006	0.026	0.345
MIN	0.000	0.044	0.000	0.042	0.000	32.964	51.516	0.000	0.471	11.101
MAX	0.003	0.103	0.025	0.103	0.010	34.121	52.982	0.016	0.551	12.128
The Sample from Layer of massive Sn-Pb-Zn ore of No 105, level -153 m										
MEAN (38)	0.006	0.051	0.006	0.083	0.002	33.668	51.119	0.004	0.450	12.748
S.D.	0.0082	0.0178	0.0125	0.0215	0.0036	0.2786	0.2562	0.0060	0.0323	0.2818
MIN	0.000	0.000	0.000	0.039	0.000	32.964	50.617	0.000	0.389	11.240
MAX	0.060	0.094	0.056	0.128	0.016	34.007	52.074	0.019	0.520	13.090
The Sample from Layer of massive Sn-Pb-Zn ore of No 105, level -103 m										
MEAN (7)	0.004	0.070	0.004	0.096	0.004	33.267	53.539	0.001	0.533	11.029
S.D.	0.009	0.027	0.006	0.013	0.005	0.808	0.695	0.002	0.076	0.431
MIN	0.000	0.040	0.000	0.081	0.000	31.750	51.951	0.000	0.426	10.746
MAX	0.026	0.129	0.017	0.123	0.014	34.313	54.114	0.005	0.63	12.069

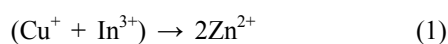
5. Discussion

5.1. Elemental Distribution and Substitution Mechanisms of Indium

Zn and In are adjacent and diagonal to each other in the periodic table, the ionic radiuses of In^{3+} and Zn^{2+} are 0.081 nm and 0.074 nm, respectively, and both have an electronegativity of 1.6. Because of this, In^{3+} can completely replace Zn^{2+} in tetrahedrons. Although the principles of the analytical

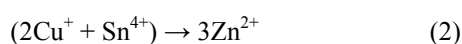
methods are totally different, the results from electron probe microanalysis are similar to the data obtained from ion-coupled plasma mass spectroscopy in terms of the limit of experimental error, indicating that indium is present homogeneously in sphalerite. There are no any inclusions were observed, for example, chalcopyrite inclusions, except that several localized spots with high concentrations of indium were present in concentration maps of indium from EPMA, such as sample TK190-1 (Figure 6). It is thus demonstrated that indium principally occurs in sphalerite by isomorphism, and is perhaps

present in nanoscale indium-rich ultra micro-inclusions in some sphalerite regions. Based on the EMPA analysis, representative relations between Cu and In are illustrated in Figure 7, with the coupled substitution mechanism



The elemental relations for sphalerite from the Dachang ore-field ore block observed herein are in good agreement with previously published data [10-11]. From the coupled substitution mechanism, the ratio of copper to indium should be 1:1, and the analytical results should lie on the 1:1 line, which is known as the copper-indium line. However, most values are lower than the line, i.e., with elevated Cu and lowered In. Orebodies No. 105 and No. 92 are the closest to the line; orebody No. 95 completely deviates from the copper-indium line.

Observations made under the microscope and concentration maps of indium from EPMA show that sphalerite contains large numbers of microscopic chalcopyrite inclusions. The analytical results will plot lower than the Cu-In line when the diameter of the EPMA beam spot is greater than the diameter of the inclusions, because Cu will be partly supplied by chalcopyrite inclusions as well as isomorphism of sphalerite. Moreover, Hiroyasu and Shunso [21] proposed that copper together with tin can substitute for zinc,

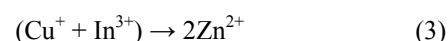


In addition to indium. The results of the electron

microprobe and ICP-MS analyses indicate the presence of tin in sphalerite. The existence of tin in sphalerite can also cause test results to plot below the copper-indium line. When the concentration of copper is greater than its solubility in sphalerite, chalcopyrite will be exsolved. This is the reason why sphalerite contains large amounts of chalcopyrite. From this, the presence of chalcopyrite inclusions and tin can lead to deviation from the copper-indium line. The majority of the copper in sphalerite is present as the result of coupled substitution of zinc with indium but, because of the above two factors, the majority of analytical results are near or below the copper-indium line.

As the indium concentration in orebody No. 95 is very low, the analytical results are almost zero. The four points located above the copper-indium line indicate that the indium concentration is more than isomorphous. It is likely that indium exists in the form of ultra-microscopic (nanometer-scale) inclusions, which is consistent with the presence of high-indium spots in indium concentration maps. Further work should be undertaken to confirm the existence of nanoscale indium inclusions.

In summary, the major occurrence form of indium in sphalerite is isomorphism with the coupled substitution mechanism



But this does not exclude the possibility that some occurs as sub-microinclusion.

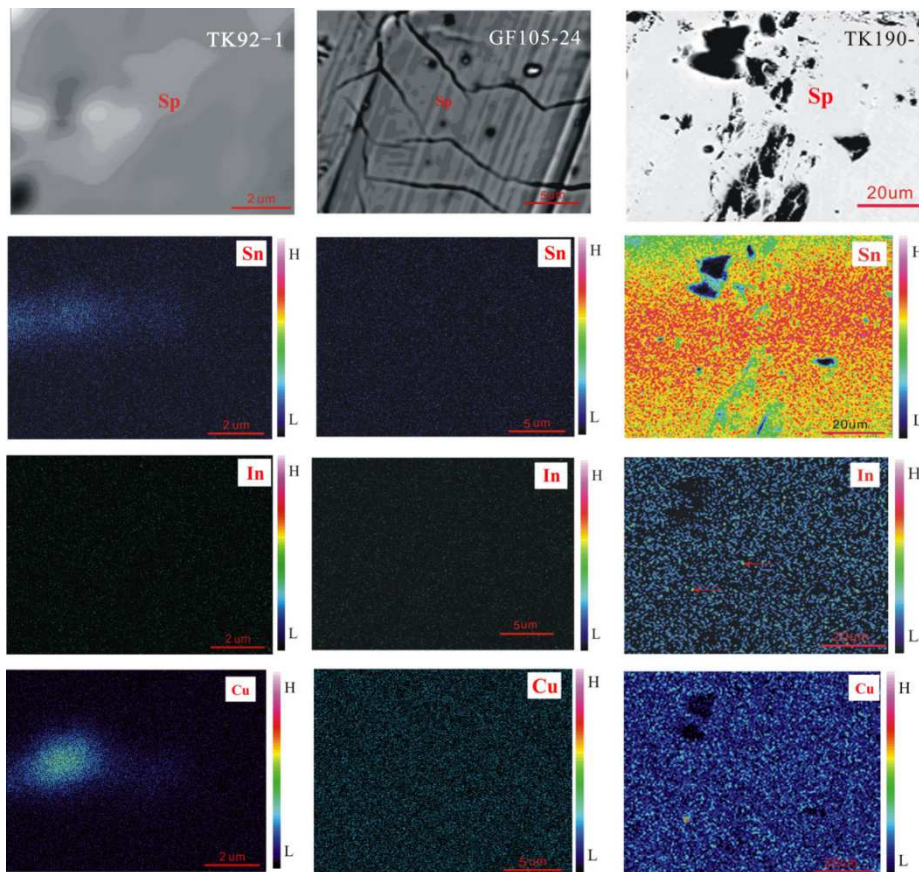


Figure 6. Images consisting of backscattered image and qualitative microprobe images of In, Cu, Sn and Cd for sphalerite.

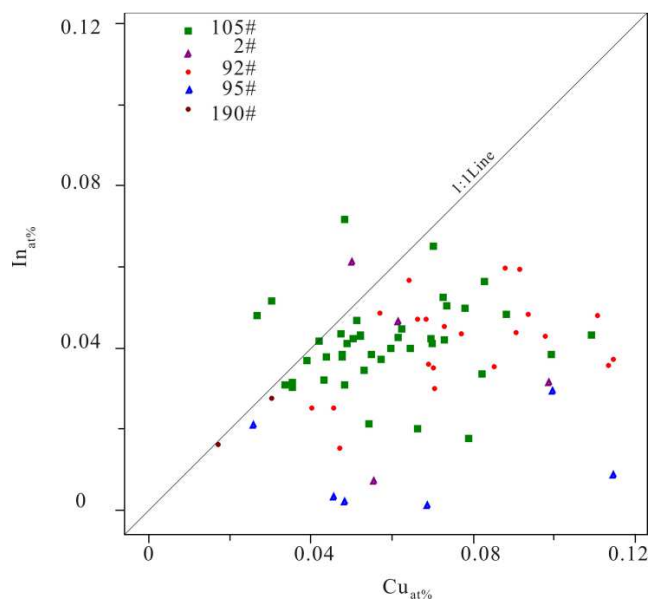


Figure 7. Relationships between In and Cu for sphalerite.

5.2. Relationship Between In, Sn and Cd in Dachang Sphalerite

Previous research has suggested that indium-rich ore fluids are the material basis for the formation of indium-rich ore block, because the presence of tin favors movement of indium into fluid and its migration [22]. Experiments by Zhang and Hu [23] experiment confirmed that indium, together with tin, is migrated and enriched in the gaseous state. Indium and tin may be transported in the same chlorine complex anionic form [24].

Under oxidizing conditions, tin and indium have similar geochemical properties. In hydrothermal ore, tin and indium are transported as complex anions and separate when the physical and chemical conditions change. When the deposit contains large amounts of sphalerite, indium will preferentially enter the sphalerite tetrahedron, but will move into tin sulfate minerals in the absence of sphalerite. An example of this is the Portuguese Neves Corvo tin-copper deposit, which contains stannite with almost 0.7% tin [7]. Many minerals containing indium are variants of stannite, such as indium-stannite. Therefore, indium and tin have a very close relationship.

Sphalerite containing indium is always cadmium-rich. Cadmium-rich sphalerite does not necessarily contain indium, such as in the Niujaotang cadmium deposit, but indium-containing sphalerite must contain cadmium. Harald et al. [12] proposed the concept of the “indium window” when studying the San Roque ore block, which means that the concentration of indium will be greatest for cadmium concentrations of 0.2% to 0.6% in sphalerite. In addition, that study found that indium readily occurs in tetrahedral sphalerite, but is less easily incorporated into cubic and rhombic dodecahedral sphalerite, which may be caused by the addition of cadmium and lead to the crystal structure and subsequent changes in the lattice parameters. The cadmium concentration in the Dachang deposit is about 0.4% to 0.5%, which may be because of indium enrichment.

In summary, tin can only migrate effectively in indium-rich ore-forming fluid, and indium precipitation into sphalerite requires a particular structure formed by cadmium and iron. Therefore, indium is always present in marmatite in tin polymetallic ore block that contain cadmium.

5.3. Relationships Between Indium Enrichment and Magmatite

Although the origin of the Dachang tin-polymetallic deposit is quite controversial, there is a definite relationship between magmatic rocks and mineralization in Dachang. As indium is chalcophilic and an incompatible element, most tends to remain in the residual magmatic hydrothermal fluid in late magmatic fractionation, which may be similar to the evolution of tin. Copper, indium, and tin are mainly present as chloride complexes [24]. New research results indicate that some of the Dachang metal ore block were migrated, enriched, and mineralized in gaseous form [23].

From the spatial variation, the concentrations of copper, indium, and tin in sphalerite decrease with depth in the Tongkeng deposit (Figure 5). As the intrusion is located in the deep part of the orebody, magmatic ore fluid migrated upward along favorable tectonic zones, and became enriched and mineralized when the physical and chemical conditions changed. This can explain the spatial variation of copper, indium, and tin in sphalerite. Elements such as iron and cadmium have completely different geochemical behavior to copper, indium, and tin, which indicates that the source and enrichment conditions of the two groups of elements are completely different. In addition, the variation in ore-forming elements in the section through the Tongkeng deposit indicates that the Tongkeng deposit is closely related to the underlying igneous rocks. Orebody No. 105 at the top of the north-south reef collapse site was formed from late ore fluid filling. This is the reason why the indium and cadmium concentrations in the three levels of orebody No. 105 are stable.

Sphalerite often contains many trace elements such as Fe, Mn, Cd, Ga, Ge, and In, and the variation in levels provides useful information on the type and origin of mineralization in the deposit [10, 25-27]. Our results show that the Dachang sphalerite is characterized by enrichment of Fe, Mn, Cd, and In, with the levels of Fe, Mn, Cd, and other elements being relatively constant while In, Sn, Pb, Cu, and Bi have a large range of concentrations. These characteristics are distinct from those of skarn ore block that have sphalerite enriched in Co, relatively enriched in Fe, and depleted in In, Ga, and Sn [27]. The Dachang deposit also differs from MVT-type Pb-Zn ore block, such as Niujaotang, Huize, and Mengxing, which contain sphalerite enriched in Cd and depleted in In and Fe, and the Jinding Pb-Zn deposit. On the In-Fe, In-Sn, Cu-Sn, and Cd/Fe-In/Fe diagram, the points for Dachang sphalerite are all located in the hydrothermal-sedimentary lead-zinc ore block area, which is related to late Yanshanian magmatic hydrothermal alteration. This indicates that the indium in Dachang has a close relationship with magmatic evolution (Figure 8).

Indium-bearing ore block are associated with late magmatic

evolution throughout the world. Thomas and Dirk [15] indicated that an indium-rich orebody was closely related to emplacement of post-collisional lamprophyric and rhyolitic dikes. Sinclair *et al.* [28] showed that enrichment of indium and late generation of granitic porphyritic rocks or beads were closely linked in the Mount Pleasant tin-polymetallic deposit of Canada. Shimizu and Aoki [29] determined the Toyoha-Muine metallogenic period using the K-Ar method, and concluded that indium generation was related to the latest intrusive rocks. Therefore, indium enrichment is closely related to late-stage magmatic evolution, which may be veins or rock beads.

The main rock types in the Dachang deposit are the Longxianggai pluton and porphyritic or granitic diorite veins. The Longxianggai pluton is a multi-stage intrusion in the middle of the Dachang ore field. The pluton formed in three stages.

The ages for granite porphyry (91 ± 1 Ma) and diorite dikes (91 ± 1 Ma) obtained by Cai *et al.* [30] indicate that the granite porphyry and diorite dikes occurred later than the formation of the Longxianggai pluton. Meanwhile, field observations showed that the granite porphyry is cut by ore veins (Figure 2), indicating that porphyry diagenesis occurred during the significantly late to main mineralization stage.

From the ore textures of the Gaofeng and Tongkeng ore block in Dachang, there were two stages of mineralization. In the main mineralization, the early stage was dominated by cassiterite and there was a great deal of metasomatism. In the late stage, chalcopyrite and pyrite veins infilled the cleavage or fracture in the sphalerite that formed in the previous stage.

From the discussion above, there is a close relationship between copper and indium. Therefore, the indium may have been deposited in the late mineralization stage, which agrees with findings for the Toyoha deposit of Japan and the Mount Pleasant deposit of Canada [28]. From the relationship between the formation of indium ore block worldwide and the dikes generated in late-stage magmatic evolution, combined with the significant increase of chalcopyrite in sphalerite on both sides of the dikes, it can be inferred that the indium enrichment during the late stage was closely related to granite porphyry dikes generated in late magmatic evolution.

From the relationship between indium and copper, we can infer that indium may have been enriched by the ore-fluid that was generated by the late porphyry intrusion of the Dachang magmatic evolution and was rich in copper, indium, and tin. The indium enrichment process of Dachang was similar to that of other indium ore block worldwide. For example, in the Toyoha indium deposit of Japan, indium-containing sphalerite was generated from non-indium-containing sphalerite that was altered by late fluid enriched in indium, copper, tin, and silver, and the indium occurs in the tinge bands of sphalerite.

In summary, the enrichment of indium in sphalerite has a close connection with the granite porphyry formed during late magmatic evolution. The indium in early sphalerite was enriched as a result of alteration by indium-rich fluid, but the process of Cd enrichment was different from that of In, which emphasizes the spatial variation of Cd, Cu, and In. However, the addition of Cd to sphalerite provides a path for indium migration.

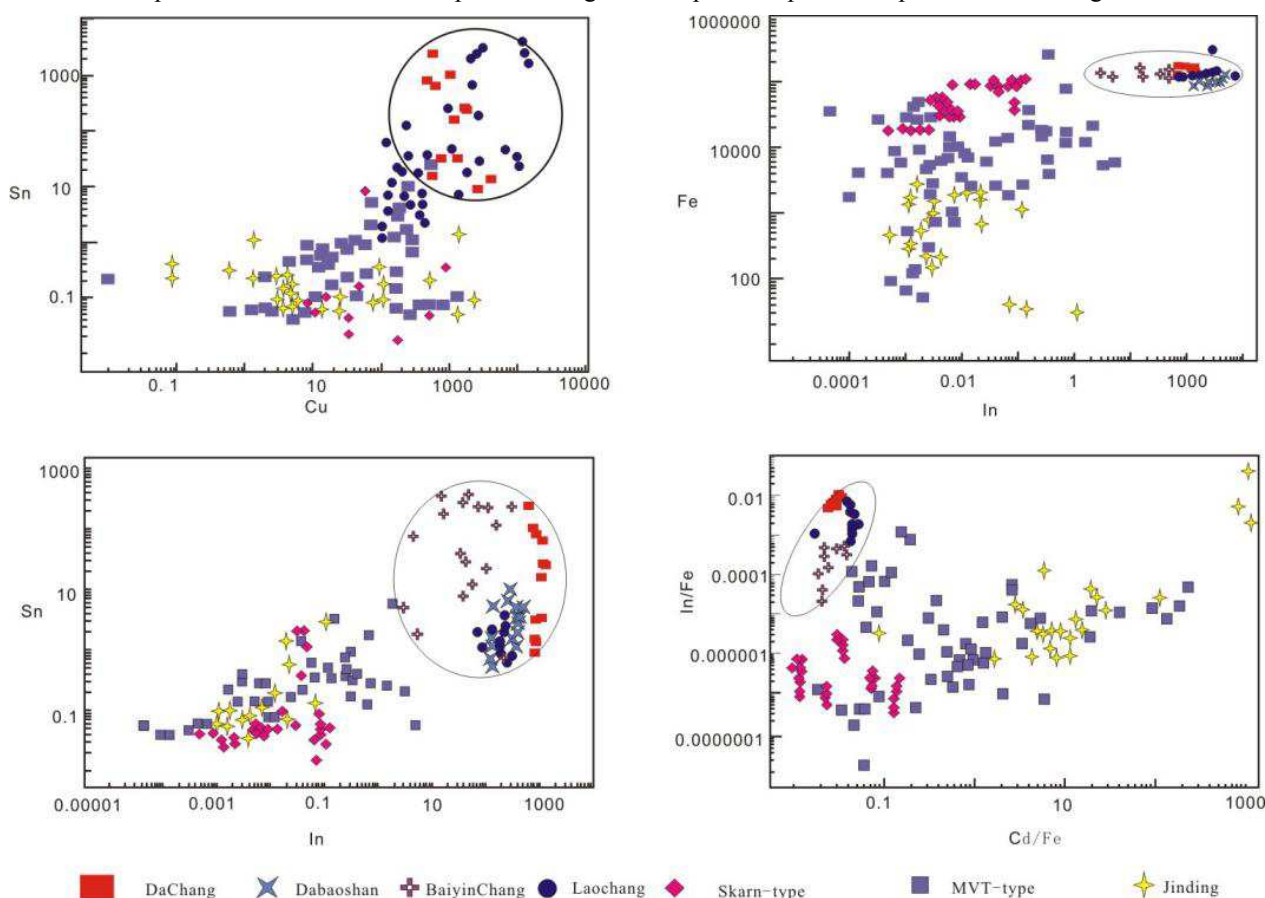


Figure 8. Binary plots of In vs. Fe, In vs. Sn, (Cu + Ag) vs. (In + Sn), Cd/Fe vs. In/Fe in sphalerite from Dachang and other Pb-Zn deposits in China.

6. Conclusions

From systematic sampling of different levels of the Tongkeng and Gaofeng deposit in Dachang and analysis of the variation of major elements in indium-sphalerite, we found that the concentrations of copper, indium, and tin decrease with increasing depth, but the iron and cadmium levels remain unchanged.

Indium in sphalerite mainly occurs isomorphically, but some may be present in ultra-microscopic inclusions, the substitution being $\text{In}^{3+} + \text{Cu}^+ \rightarrow 2\text{Zn}^{2+}$. From electron microprobe analysis of the mineral phases and surface features, the enrichment of indium occurred as a result of transport into sphalerite through alteration by copper and indium-rich fluid.

The indium enrichment has a close relationship with late-stage granite porphyry intrusions Dachang. Thus, granite porphyry dikes are significant indicators for indium deposit in tin-rich polymetallic mine zones.

Acknowledgements

Many thanks go to Professor Zheng Zhuanlun and Professor Lei Liangqi of Guilin University of Technology. This research was supported jointly the National Science Foundation of China (41563004 and 41674075).

References

- [1] Zhan, H., Hu, J. G., Cai, M. H., Shao, Z. Z., Liu, J. X., Hu, Z. W. Occurrence characteristics of trace elements in sphalerite of Tongkeng indium-rich tin deposit, Guangxi. *Science Technology and Engineering*. 2019, 19 (19): 34-45.
- [2] Tao, Y., Hu, R. Z., Tang, Y. Y., Ye, L., Qi, H. W., Fan, H. F. Types of dispersed elements bearing ore-deposits and their enrichment regularity in Southwest China. *Acta Geologica Sinica*. 2019, 93 (6): 1210-1230.
- [3] Pat Shanks, III. W. C., Kimball, B. E., Tolcin, A. C. Germanium and indium. U.S. Geological Survey. Professional Paper. 2017, 1802: I1-I27.
- [4] Tang, Y., Bi, X., Fayek, M., Stuart, F. M., Wu, L., Jiang, G., Xu, L., Liang, F. Genesis of the Jinding Zn-Pb deposit. Northwest Yunnan Province, China: Constraints from rare earth elements and noble gas isotopes. *Ore Geology Reviews*. 2017, 90: 970-986.
- [5] Xu, J., Li, X. F. Spatial and temporal distributions, metallogenic backgrounds and processes of indium deposits. *Acta Petrologica Sinica*. 2018, 34 (12): 3611-3626 (in Chinese with English abstract).
- [6] Ishihara, S., Murakami, H., Marquez-Zavalia, M. F. Inferred indium resources of the Bolivian tin-polymetallic deposits. *Resource Geology*. 2011b, 61: 174-191.
- [7] Benzaazoua, M., Marion, L. P., Pinto, A. Tin and indium mineralogy within selected samples from the Neves Corvo ore deposit (Portugal): A multidisciplinary study. *Mineral Eng*. 2003, 16 (11, suppl 1): 1291-1302.
- [8] Yang, R. D., Gao, J. B., Zhao, K., Yu, J. L., Zhu, C. L., Gao, L., Chen, J. Y., Zhou, R. X. Roof and floor characteristics of bauxite in Qingzhen Guizhou and their implication for bauxite mineralization. *Acta Petrologica Sinica*. 2018, 92 (10): 2155-2165 (in Chinese with English abstract).
- [9] Ye, L., Liu, Y. P., Zhang, Q., B, T., H, F., W, X. J. Trace and rare earth elements characteristics of sphalerite in Dulong super large Sn-Zn polymetallic ore deposit, Yunnan Province. *Journal of Jilin University: Earth Science Edition*. 2017, 47 (3): 734-750 (in Chinese with English abstract).
- [10] Ye, L., Cook, N. J., Ciobanu, C. L. Trace and minor elements in sphalerite from base metal deposits in South China: LA-ICPMS study. *Ore Geology Review*. 2012a, 39: 188-217.
- [11] Cook, N. J., Ciobanu, C. L., Pring, A. Trace and minor elements in sphalerite: A LA-ICPMS study. *Geochimica et Cosmochimica Acta*. 2009, 73: 4761-479.
- [12] Harald, G. D., Mirta, M. M., Frank, M. Sulfidic and non-sulfidic indium mineralization of the epithermal Au-Cu-Zn-Pb-Ag deposit San Roque (Provincia Rio Negro, SE Argentina) - with special reference to the "indium window" in zinc sulfide. *Ore Geology Reviews*. 2013, 52: 103-128.
- [13] Zhang, J. R., Wen, H. J., Zou, Z. C. Ore-forming fluid characteristics of the Jinman vein-type copper deposits in the western Lanping basin and its metallogenic significance. *Journal of Jilin University: Earth Science Edition*. 2017, 47 (3): 706-718 (in Chinese with English abstract).
- [14] Bi, X. W., Tang, Y. Y., Tao, Y. Composite metal logogenesis of sediment hosted Pb-Zn-Ag-Cu base metal deposits in the Aanjian collisional orogen, SW China, and its deep driving mechanisms. *Acta Petrologica Sinica*. 2019, 35 (5): 1341-1371 (in Chinese with English abstract).
- [15] Li, X. F., Yang, F., Chen, Z. Y. A tentative discussion on geochemistry and genesis of indium in Dachang tin ore district, Guangxi. *Mineral Deposits*. 2010, 29 (5): 903-914 (in Chinese with English abstract).
- [16] Leng, C. B., Qi, Y. Q. Genetic constraints of Lengshuikeng Ag-Pb-Zn ore field in Jiangxi: constraint from LA-ICPMS analyses of minor and trace element in sphalerite and galena. *Acta Petrologica Sinica*. 2017, 91 (10): 2256-2272 (in Chinese with English abstract).
- [17] Deng, J., Wang, Q. F., Li, G. J. Super imposed orogeny and composite metallogenic system: Case study from the Sanjiang Tethyan belt, SW China. *Acta Petrologica Sinica*. 2016, 32 (8): 2225-2247 (in Chinese with English abstract).
- [18] Tao, Y., Putirka, K., Hu, R. Z. The magma plumbing system of the Emeishan large igneous province and its role in basaltic magma differentiation in a continental magma differentiation in a continental setting. *American Mineralogist*. 2015, 100 (11/12): 2509-2517.
- [19] Li, Y. B., Tao, Y., Zhu, F. L. Distribution and existing state of indium in the Gejiu tin polymetallic deposit, Yunnan, SW China. *Chinese Journal of Geochemistry*. 2015, 34 (4): 469-483.
- [20] Liang, T., Wang, D. H., Hou, K. J. LA-MC-ICP-MS zircon U-Pb dating of Longxianggai pluton in Dachang of Guangxi and its geological significance. *Acta Petrologica Sinica*. 2011, 27 (1): 1624-1636 (in Chinese with English abstract).

- [21] Hiroyasu, M., Shunso, I. Trace elements of Indium-bearing sphalerite from tin-polymetallic deposits in Bolivia, China and Japan: A femto-second LA-ICPMS study. *Ore Geology Reviews*. 2013, 53: 103-128.
- [22] Zhu, X. Q., Zhang, Q., He, Y. L., Zhu, C. H. Relationships between indium and tin, zinc and lead in ore-forming fluid from the indium-rich and -poor deposits in China. *Geochimica*. 2006, 35 (1): 6-12 (in Chinese with English abstract).
- [23] Zhang, R. H., Hu, S. M. The evolution of deep earth fluids and ore genesis. *Earth Science Frontiers*. 2001, 8 (4): 297-310 (in Chinese with English abstract).
- [24] Wood, S. A., Samson, I. M. The aqueous geochemistry of gallium, germanium, indium and scandium. *Ore Geology Review*. 2006, 28: 57-102.
- [25] Ishihara, S., Endo, Y. Indium and other trace elements in volcanogenic massive sulphide ores from the Kuroko, Besshi and other types in Japan. *Bulletin. Geological Survey of Japan*. 2007, 8: 7-22.
- [26] Wang, C. M., Deng, J., Zhang, S. T., Xue, C. J., Yang, L. Q., Wang, Q. F., Sun, X. Sediment-hosted Pb-Zn deposits in Southwest Sanjiang Tethys and Kangdian area on the western margin of Yangtze Craton. *Acta Geologica Sinica*. 2010, 84 (6): 1428-1438.
- [27] Ye, L., Gao, W., Yang, Y. L., Liu, T. G., Peng, S. S. Trace elements in sphalerite in Laochang Pb-Zn polymetallic deposit, Lancang, Yunnan Province. *Acta Petrologica Sinica*. 2012b, 28 (5): 1362-1372 (in Chinese with English abstract).
- [28] Sinclair, W. D., Kooiman, G. J. A. Geochemistry and mineralogy of indium resources at Mount Pleasant, New Brunswick, Canada. *Ore Geology Reviews*. 2006, 28: 123-145.
- [29] Shimizu, T., Aoki, M. Hydrothermal alteration and K-Ar ages of Neogene Quaternary magmatic hydrothermal systems at Toyoha-Muibe area in southwest Hokkaido, Japan. *Resource Geology*. 2011, 61: 192-209.
- [30] Cai, M. H., He, L. Q., Liu, G. Q., Wu, D. C., Huang, H. M. SHRIMP zircon U-Pb dating of the intrusive rocks in the Dachang tin-polymetallic ore field, Guangxi and their geological significance. *Geological Review*. 2006, 52 (3): 409-414 (in Chinese with English abstract).